A TWO-DIMENSIONAL SYNTHETIC APERTURE RADAR IMAGING SIMULATION OF MOVING OCEAN WAVES

Koichiro Wakasugi, Naru-fumi Kishi, and Masaru Matsuo

Department of Electrical Engineering
Kyoto Institute of Technology
Matsugasaki, Kyoto 606, Japan

ABSTRACT

An analytic model of the ocean surface SAR images with a more realistic three-dimensional framework is presented under the assumption that a trochoidal swell propagates through a uniform field of Bragg-type distributed scatterers. Two-dimensional SAR images are calculated for the interpretation and prediction of actual SAR images of the ocean surface as a function of ocean wave amplitude, wave frequency, propagation direction and radar frequency, off-nadir angle of the antenna, and spatial resolutions.

1. INTRODUCTION

The spaceborne synthetic aperture radar (SAR) has opened up a new dimension in our capability to study the ocean because it provides synoptic radar images with high resolution in short time [Tomiyasu, 1978; Beal et al., 1981]. However, it is controversial as to what physical mechanism is causing the formation on SAR imaging of the ocean surface [Elachi and Brown, 1977; Valenzuela, 1980; Harger, 1983]. The radar cross section modulation by the long ocean waves is responsible for the image formation, especially for a real aperture radar. Since the SAR uses the Doppler history of echoes to achieve its high resolution, the orbital motion of water particles can also play a dominant role in SAR image formation [Swift and Wilson, 1979; Alpers and Rufenach, 1979].

This paper discusses a two-dimensional SAR imaging based on the treatment of Swift and Wilson [1979]. The calculations assume that a trochoidal ocean gravity wave propagates a uniform field of Bragg-type distributed scatterers. Since three dimensions are considered in our model, two-dimensional SAR images can be obtained as a function of ocean wave amplitude, wave frequency, direction of wave propagation and radar frequency, off-nadir angle of the antenna, and spatial resolutions in azimuth and range. The analytic model with a more realistic three-dimensional framework will be a help for the interpretation and prediction of actual SAR images of the ocean surface.

2. THEORY

Let us consider a line source in circular motion, as shown in Fig.1. The line source is moving in a circle of radius α and with angular velocity ω_c, and the axis of rotation is perpendicular to the wave propagation direction. The motion of a point on the line whose center is at $(x_c, y_c, 0)$ is given by

$$\begin{aligned} x(t) &= x_c - \alpha \cos\theta \sin(\phi - \omega_c t) \\ y(t) &= y_c - \alpha \sin\theta \sin(\phi - \omega_c t) \\ z(t) &= \alpha \cos(\phi - \omega_c t) \end{aligned} \qquad (1)$$

where ϕ and θ represent the initial location of the line source and the angle of the wave propagation relative to the x axis. The SAR is moving along the x axis with velocity v, altitude h. If $R(x_0, y_0, t)$ is the distance between the SAR and the point, it is then approximated as

$$R(x_0, y_0, t) \sim R_0 + \frac{1}{2R_0}[(x_0 - vt)^2 - 2\alpha_z h \cos(\phi - \omega_0 t) - 2\alpha_y y_0 \sin\theta \sin(\phi - \omega_0 t)] \quad (2)$$

where $\alpha_z = \alpha_y = \alpha$; the subscripts Z and Y are used for discriminating the motion components associated with the altitude and the range directions, respectively. We assume $(x_0 - vt)/R_0 \ll 1$ and $\alpha/R_0 \ll 1$ in deriving Eq.2, and R_0 is the distance between the SAR and the center of the antenna footprint (i.e., $R_0^2 = h^2 + y_0^2$).

The trochoidal wave train is assumed to propagate through a field of scatterers with a distributed cross section $\sigma(x_0, y_0)$ [LeBlond and Mysak, 1980]. Since the phase history is given by $\exp[2iKR(x_0, y_0, t)]$ (K: radar wavenumber), the SAR signal processing gives a two-dimensional image intensity I(x,y) as follows:

$$I(x,y) = \int |F_R(y_0, y)|^2 \cdot \int \sigma(x_0, y_0) |F_A(x_0, y_0, x)|^2 \, dx_0 \, dy_0 \quad (3)$$

where F_R and F_Y are the azimuthal and range response functions of a moving point centered at $(x_0, y_0, 0)$. These functions depend on ocean wave parameters such as wave amplitude α, wave frequency ω_0, propagation direction θ and on radar system parameters such as radar wavenumber K, off-nadir angle of the antenna δ_0, and azimuthal and range resolutions ε_x and ε_y. Since we neglect the cross section modulation, $\sigma(x_0, y_0)$ is assumed to be unity for the following discussions.

Fig.2 shows an example of SAR images representing a region of ± 1.0 km in azimuth and range directions. For the calculations, the SEASAT SAR parameters are chosen [Jordan, 1980]; the resolutions ε_x and ε_y are fixed at 25 m and the radar wavelength is chosen as 0.25 m (L-band). The SAR moves at an altitude of 800 km with a speed of 8 km s^{-1}. The ocean wave is assumed to be a swell of 250 m in wavelength L_0 ($L_0 = 2\pi g / \omega_0^2$). The figure shows a formation of wave-like patterns even for a uniform radar scattering cross section. This is due to the velocity bunching as was noted by several authors [Elachi and Brown, 1977; Alpers and Rufenach, 1979; Swift and Wilson, 1979]. Parametric calculations are conducted as a function of wave propagation direction θ, off-nadir angle δ_0, and a normalized wave amplitude $\zeta = \alpha / L_0$ in the following section.

3. DISCUSSIONS AND CONCLUDING REMARKS

Since three dimensions are considered in our model, we can examine the effects of ocean and radar parameters on SAR images in a more realistic framework.

Fig.3 illustrates the maximum azimuthal shift of scatterers in image plane as a function of the radar off-nadir angle δ_0 and of the ocean wave direction θ. The shift is normalized by $L(\theta) = L_0 / \cos\theta$, an equivalent azimuthal wavelength of the ocean wave. The shift increases

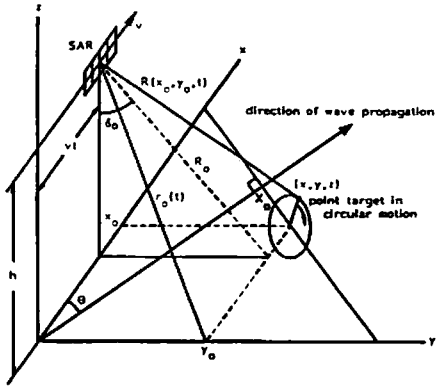

Fig.1. Geometry of synthetic aperture radar imagery.

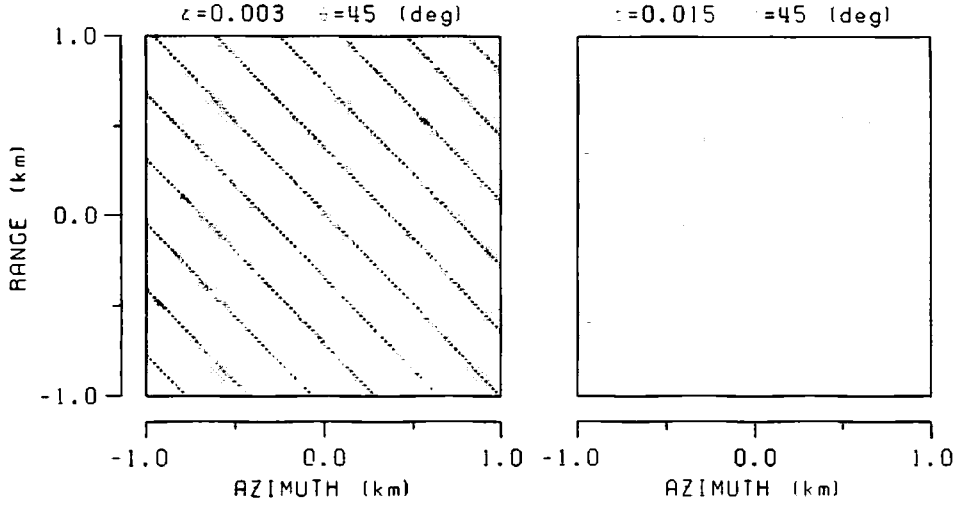

Fig.2. Examples of SAR image calculated for different amplitude of the ocean wave.

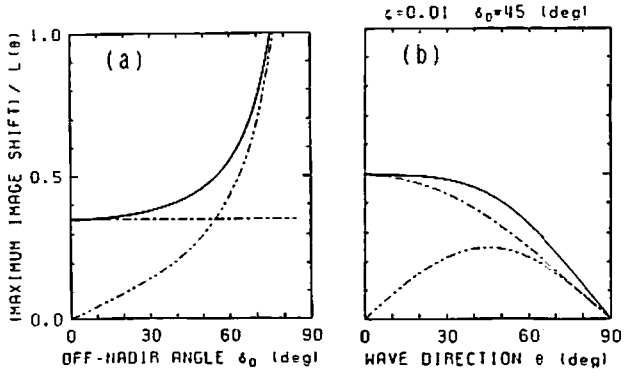

Fig.3. Dependence of the maximum azimuthal image shifts on (a) the radar off-nadir angle δ_0 and (b) the wave direction θ.

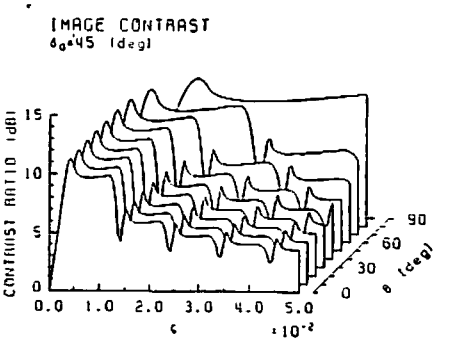

Fig.4. Dependence of SAR image contrast on the amplitude ζ and the wave direction θ.

as the off-nadir angle increases, as shown in Fig.3(a). This is mostly due to the y-component of motions, and the z-component produces a constant image shift which is determined only by the normalized wave amplitude ζ. The dependence on the wave direction θ is illustrated in Fig.3(b). Although the actual shift by the y-component increases with θ, the equivalent wavelength, $L(\theta)$, also increases and the normalized shift becoming a maximum at $\theta = 45°$. Fig.3 shows that the amount of shifts is generally within a half of the equivalent wavelength $L(\theta)$, but it is large enough compared with the spatial resolutions of the SAR considered.

Fig.4 shows the dependence of SAR image intensity on the amplitude and direction of the ocean wave. The ordinate is a contrast ratio which is defined as an intensity ratio of the minimum to the maximum of the calculated SAR images. While the azimuthal shifts are proportional to the wave amplitude ζ, the image contrast is determined by the degree of scatterer's bunching. Therefore, the figure shows a strong contrast by $\sim$10 dB when the wave amplitude ζ is relatively small or when the direction of ocean wave θ approaches the right angle.

In the present work, we have emphasized the effects of trochoidal wave motions on SAR imaging formation with a more realistic three-dimensional framework. SAR images are calculated as a function of actual ocean and radar parameters. The image contrast is estimated to be several to 10 dB, which is comparable to the value expected by a cross section modulation due to the long waves [Elachi and Brown, 1977]. This modulation effect dominates for ocean waves propagating perpendicular to the SAR flight direction. However the azimuthal shifts are several times larger than the spatial resolutions of the SAR as was shown in Fig.3, it is relatively simple to take into account the modulation effect through the radar cross section $\sigma(x_0, y_0)$ for the present analytic framework.

REFERENCES

W.R.Alpers and C.L.Rufenach, "The effect of orbital motion on synthetic aperture radar imaging of ocean waves," IEEE Trans. Antennas Propagat., vol.AP-27, pp.685-690, 1979.

R.C.Beal, P.S.DeLeonibus, and I.Katz (ed), Spaceborne synthetic aperture radar for oceanography, Johns Hopkins Univ. Press, Baltimore, MD, 1981.

C.Elachi and W.E.Brown, "Models of radar imaging of ocean surface waves," IEEE Trans. Antennas Propagat., vol.AP-25, pp.84-95, 1977.

R.O.Harger, "Inverting a dispersive scene's side-scanned image," Radio Sci., vol.18, pp.83-92, 1983.

R.L.Jordan, "The Seasat-A synthetic aperture radar system," IEEE J.Oceanic Eng., OE-5, pp.154-164, 1980.

P.H.LeBlond and L.A.Mysak, Waves in the ocean, Elsevier, Amsterdam, 1980.

C.Swift and L.R. Wilson, "Synthetic aperture radar imaging of moving ocean waves, "IEEE Trans. Antennas Propagat., vol.AP-27, pp.725-729, 1979.

K.Tomiyasu, "Tutorial review of synthetic aperture radar (SAR) with applications to imaging of the ocean surface," Proc. IEEE, vol.66 pp.563-583, 1978.

G.R.Valenzuela, "Theories for the interaction of electromagnetic and ocean waves," Boundary Layer Met., vol.13, pp.61-85,1978.

G.R.Valenzuela, "An asymptotic formulation for SAR images of dynamical surface," Radio Sci., vol.15, pp.105-114, 1980.